

Towards the Development of Robo-Aide: A Robotic Arm to Foster Independent Living for People with Mobility Impairments

23rd April 2018

Joanna Deaton, Benjamin Flamm

BMED 4739 - Medical Robotics

School of Biomedical Engineering, Georgia Institute of Technology
Atlanta, Georgia

Abstract—The ability to walk or reach an object on the top shelf is a privilege that people take for granted every single day. When someone is no longer capable of performing simple tasks around the house, a home health aide is the usual solution to assist with everyday life. Mobility has been shown to be the most common disability among the elderly with millions of citizens in the U.S. alone requiring help with household tasks. Although they are considered necessary, these professions that support immobilized patients have expensive rates. This paper introduces the prototype for an autonomous robotic arm that is able to accept a command to retrieve an object through voice input, use machine vision in conjunction with an attached camera to navigate its environment, locate and fetch the object, and return it to the user. Influenced by previous projects and research, the manipulator presented in this document could also be applied beyond the field of independent living; however, with the rise in aging population of baby-boomers and the deficiency of nurses in the workforce create a need for jobs such as proffering tools in the operating room to be filled. The target of this Robo-Aide is to provide a cost-efficient, un-intrusive, and consistent solution to improving the quality of life at home for people with mobility impairments or medical instrument identification and retrieval.

I. INTRODUCTION

According the U.S. Census Bureau, physical immobility is the most common disability among older Americans aged 65 and above [1]. This generation is expected to double over the next 40 years; increasing to 96 million citizens and making the percentage of their share of the general population approximately 10 percent higher [2]. With advances in modern medicine and a better healthcare system, life expectancy rates have no choice but to increase. Over the next few centuries, this relationship will cause the exponential growth of the older population and result in a more tragic state of independent living than today. This, of course, only being if systems are not invented to enable senior citizens to live at home without a health aid or any other assistance. Currently, family members

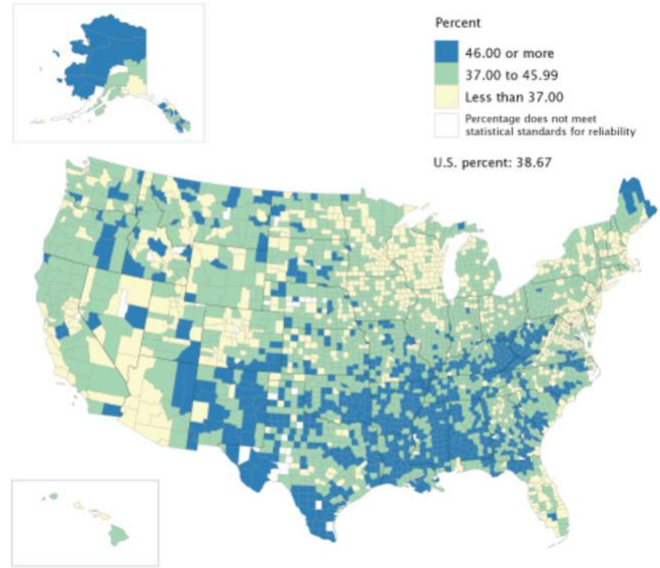


Fig. 1. Percentage of people aged 65 and above with a mobility disability by county [1].

or home health aides are the primary help for the elderly to lead more independent lives around their homes. Family members are the best choice since they are inexpensive and feel less invasive, but having to take care of a loved one can make the immobilized person seem like a burden to the helping family. This problem is solved with a home health agency, but other issues arise such as invasions of privacy, lack of standardized training, and inconsistent or even improper treatment [3][4]. In lieu of all of these flaws, price is the main deterrent to hiring help around the house with the average yearly rate at \$20,000 [5]. Novel systems such as the Human Support Robot (HSR) have been created in hopes of moving towards a solution to the issues faced in having an at-home provider; however, they are still in the earliest stages of development [6]. The HSR is limited to retrieving objects on the floor, dispensing medication, and enabling nurses or family members to check in on the patient. This design was

prototyped by Toyota only in the last year but has great potential to scale into a more autonomous robot with the ability to fetch objects from higher up places where immobilized persons may have difficulty reaching. A 3 year, NSF project in 2005 culminated in a robotic nurse called Penelope [7] [8] [9]. Penelope was developed to perform surgical technician duties around the operating room and assist the surgeon during procedures. A similar robot, called Gestonurse, was developed at Purdue in 2011 which received voice input from a surgeon, located the tool, and quickly handed it to the surgeon [10]. The surgical assistance aspect of Gestonurse involves using computer vision to locate and fetch tools to be delivered to the surgeon, but Penelope goes a step further and returns the instrument once the surgeon is finished using it. Although the application of these robotic nurses is mostly unrelated to fostering independent living in the homes of older Americans, some of her design is applicable to the prototype presented in this literature review. This paper improves on the working space of the HSR with the presentation of a prototype of an autonomous robotic arm that fosters independent living for people with mobility impairments by accepting commands to retrieve objects that may be out of reach both low and high spaces. Section II of this paper discusses the materials used in the design of the Robo-Aide, Section III discusses the methods the design analysis of the Robo-Aide, Section IV discusses the results of the current limitations and the lessons we learned for improving the Robo-Aide, and Section V discusses the conclusions and future work outlined for the prototype.

II. ROBOT MATERIALS

A. Mechanical Design

The body of the Robo-Aide is constructed using aluminum u-channels and rectangular tubes for the prismatic joints as seen in Figure 2. The vertical rectangular tube can translate up to 12.71 centimeters and the horizontal u-channel can translate up to 24.13 centimeters. These translations occur through a rack and pinion setup on the inside of the u-channels with mechanical stops cut into the each piece of aluminum to prevent the Robo-Aide from attempting to move beyond its ability. In the vertical prismatic joint, an additional gear with the same pitch angle is used to support the rack and relieve the pressure of the gear of the vertical prismatic joint that is being driven. A ball joint is used to support the rack of the horizontal prismatic joint. A metal turntable is connected to the revolute joint of the Robo-Aide through 3-D printed parts. These parts are specifically designed to fit on top of the vertical prismatic joint and be attached to the horizontal prismatic joint using small bolts as shown in Figure 3. A metal turntable is also bolted in between the 3-D

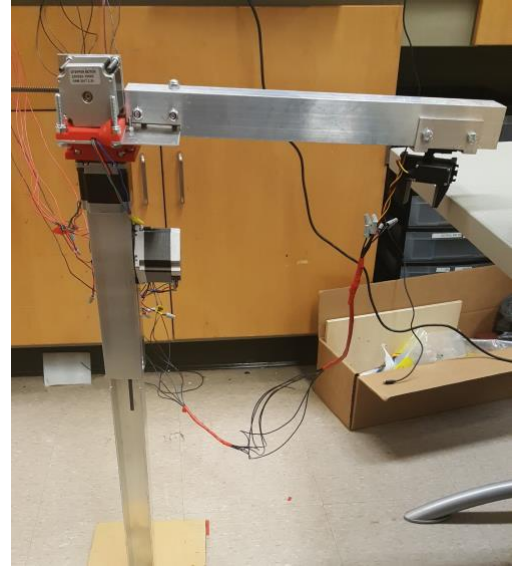


Fig. 2. Picture showing Robo-Aide structure.

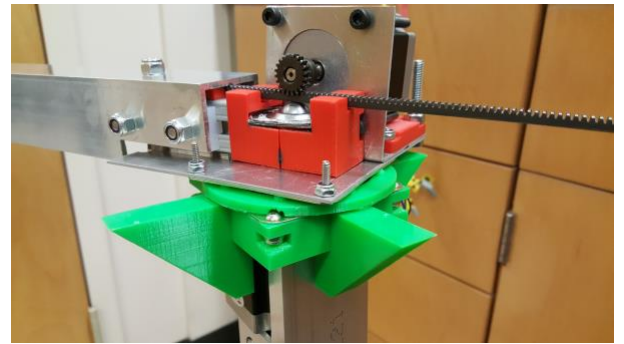


Fig. 3. 3D printed part created to support revolute joint.

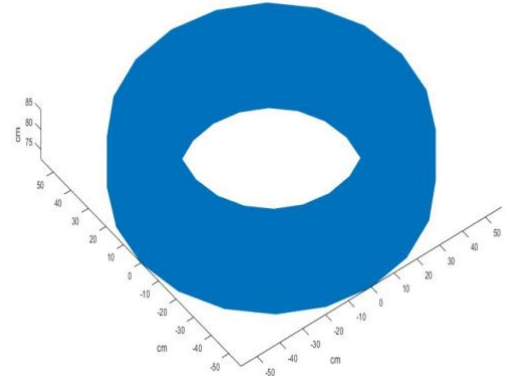


Fig. 4. Volume of end-effector workspace.

printed parts of both joints. The theoretical workspace of this design is shown in Figure 4.

B. Electrical Design

The primary power source for the Robo-Aide is the Meanwell LRS-350-5 AC/DC converter that can supply up to approximately 48 Volts [11]. The microcontroller used is the Arduino Mega2560 with an Adafruit Motorshield v2.3 attached [12] [13]. The Arduino is programmed through its own integrated development environment (IDE) to declare output signals for the stepper motor driver and claw end-effector. There are 3 motors in the design where each are Nema 23 bipolar steppers that are rated at 5 Volts and 2.8 Amps of input current [14]. These steppers are driven by 3 TB6600 stepper motor drivers that are powered by 41 Volts and interfaced to the Arduino to receive pulse and direction signals [15]. A Lynxmotion Little Grip Kit is used as the end-effector and is controlled by servo motors that also interfaces with the motor shield servo pins [16].

III. KINEMATICS AND VELOCITY

A. Derivation of the Forward Kinematics

The information in this section discusses the mathematical concepts behind the current implementation of the Robo-Aide joint configurations both while resting and retrieving an object. This implementation could be useful in an operating room where the tools the Robo-Aide is to retrieve are consistently placed in the same layout during each session. The Robo-Aide consists of 4 joints in the order prismatic, revolute, prismatic, revolute for which the home configuration and associated frames are shown in Figure 5. The DH parameters listed in Table 1 were determined using this configuration. All common perpendiculars are zero. Also, all theta offsets are zero.

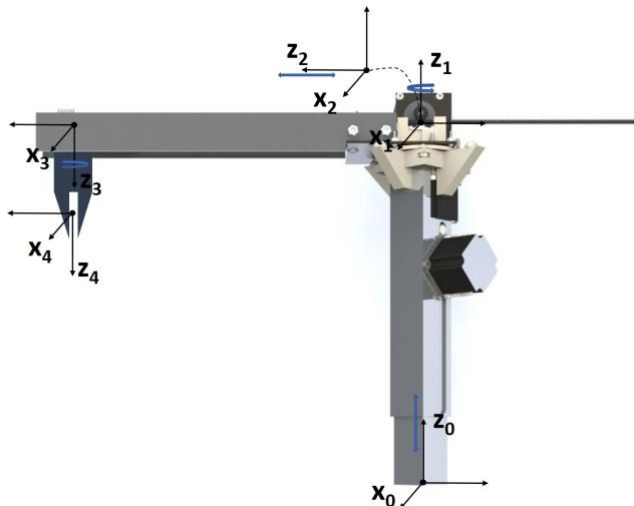


Fig. 5. SolidWorks rendering showing Robo-Aide home configuration and joint frame orientations.

Link	a	α	d	Θ	Range
1	0	0	d_1^{var}	0	0-12.71 cm
2	0	90°	0	θ_2^{var}	0°-360°
3	0	90°	d_3^{var}	0	0-24.13 cm
4	0	0	7cm	θ_4^{var}	0°-180°

Table 1. Robo-Aide DH parameter table with ranges for movement of variable joint parameters.

During the testing of the Robo-Aide, the forward kinematics could be used to determine where a specific tool should be placed in order to be picked up by the robotic arm which was hard-coded to perform a sequence of movements with set distances. The following equations for u_i , v_i , and s_i were used for rotation for each link about the z and x-axis respectively of its joints

$$u_i = \begin{bmatrix} C_i & -S_i & 0 \\ S_i & C_i & 0 \\ 0 & 0 & 1 \end{bmatrix} \quad v_i = \begin{bmatrix} 1 & 0 & 0 \\ 0 & C_i & -S_i \\ 0 & S_i & C_i \end{bmatrix} \quad s_i = \begin{bmatrix} a_i \\ 0 \\ d_i \end{bmatrix}$$

where i is the Link number in the DH parameter table. This yielded the following matrices which can be used to calculate the forward kinematic solution where I is the identity matrix:

$$u_1 = v_1 = u_3 = v_4 = I$$

$$u_2 = \begin{bmatrix} C_2 & -S_2 & 0 \\ S_2 & C_2 & 0 \\ 0 & 0 & 1 \end{bmatrix} \quad v_2 = \begin{bmatrix} 1 & 0 & 0 \\ 0 & 0 & -1 \\ 0 & 1 & 0 \end{bmatrix}$$

$$v_3 = \begin{bmatrix} 1 & 0 & 0 \\ 0 & 0 & -1 \\ 0 & 1 & 0 \end{bmatrix} \quad u_4 = \begin{bmatrix} C_4 & -S_4 & 0 \\ S_4 & C_4 & 0 \\ 0 & 0 & 1 \end{bmatrix} \quad s_1 = \begin{bmatrix} 0 \\ 0 \\ d_1 \end{bmatrix} \quad s_2 = \begin{bmatrix} 0 \\ 0 \\ 0 \end{bmatrix} \quad s_3 = \begin{bmatrix} 0 \\ 0 \\ d_3 \end{bmatrix} \quad s_4 = \begin{bmatrix} 0 \\ 0 \\ 7 \end{bmatrix}$$

The vector from the origin of Frame 0 to the origin of Frame 4, the end effector frame, can be calculated using the following equations:

$$d_4^0 = s_1 + u_2 v_2 s_3 + u_2 v_2 v_3 u_4 s_4$$

$$d_4^0 = \begin{bmatrix} S_2 S_{\alpha 2} d_3 + (S_2 S_{\alpha 2} C_{\alpha 3} + S_2 C_{\alpha 2} S_{\alpha 3}) d_4 \\ -C_2 S_{\alpha 2} d_3 - (C_2 S_{\alpha 2} C_{\alpha 3} + C_2 C_{\alpha 2} S_{\alpha 3}) d_4 \\ d_1 + (C_{\alpha 2} C_{\alpha 3} - S_{\alpha 2} S_{\alpha 3}) d_4 \end{bmatrix}$$

$$d_4^0 = \begin{bmatrix} S_2 d_3 \\ -C_2 d_3 \\ d_1 - 7 \end{bmatrix}$$

where the final equation shows the simplified version after all constant DH parameter values have been entered. This allows the position of the end effector to be known based upon the values coded in for the joint variables at each position. In the current iteration of the Robo-Aide, the values of the joint variables are set and thus known for all joints. The orientation of Frame 4 can be found using the following equations:

$$R_4^0 = u_2 v_2 v_3 u_4$$

$$R_4^0 = \begin{bmatrix} C_2 C_4 + (S_2 S_{\alpha 2} S_{\alpha 3} - S_2 C_{\alpha 2} C_{\alpha 3}) S_4 \\ S_2 C_4 + (C_2 C_{\alpha 2} C_{\alpha 3} - C_2 S_{\alpha 2} S_{\alpha 3}) S_4 \\ (S_{\alpha 2} C_{\alpha 3} + C_{\alpha 2} S_{\alpha 3}) S_4 \end{bmatrix}$$

$$(S_2 S_{\alpha 2} S_{\alpha 3} - S_2 C_{\alpha 2} C_{\alpha 3}) C_4 - C_2 S_4 \quad S_2 S_{\alpha 2} C_{\alpha 3} + S_2 C_{\alpha 2} S_{\alpha 3}$$

$$(C_2 C_{\alpha 2} C_{\alpha 3} - C_2 S_{\alpha 2} S_{\alpha 3}) C_4 - S_2 S_4 \quad -C_2 S_{\alpha 2} C_{\alpha 3} - C_2 C_{\alpha 2} S_{\alpha 3}$$

$$(S_{\alpha 2} C_{\alpha 3} + C_{\alpha 2} S_{\alpha 3}) C_4 \quad C_{\alpha 2} C_{\alpha 3} - S_{\alpha 2} S_{\alpha 3} \end{bmatrix}$$

$$R_4^0 = \begin{bmatrix} C_2 C_4 + S_2 S_4 & S_2 C_4 - C_2 S_4 & 0 \\ S_2 C_4 - C_2 S_4 & -C_2 C_4 - S_2 S_4 & 0 \\ 0 & 0 & -1 \end{bmatrix}$$

$$R_4^0 = \begin{bmatrix} \cos(\theta_2 - \theta_4) & \sin(\theta_2 - \theta_4) & 0 \\ \sin(\theta_2 - \theta_4) & -\cos(\theta_2 - \theta_4) & 0 \\ 0 & 0 & -1 \end{bmatrix}$$

where the final equation shows the simplified result when all constant DH parameter values are entered. This allows the orientation of the end effector to be known based upon the values coded in for the joint variables at each position. The following is the resultant homogeneous transformation matrix:

$$H_4^0 = \begin{bmatrix} \cos(\theta_2 - \theta_4) & \sin(\theta_2 - \theta_4) & 0 & S_2 d_3 \\ \sin(\theta_2 - \theta_4) & -\cos(\theta_2 - \theta_4) & 0 & -C_2 d_3 \\ 0 & 0 & -1 & d_1 - 7 \\ 0 & 0 & 0 & 1 \end{bmatrix}$$

B. Derivation of the Inverse Kinematics

Given that the Robo-Aide is hard-programmed to using forward kinematics to retrieve the surgical instrument, the prototype of the Robo-Aide would not require inverse kinematics until the addition of the machine vision camera discussed in later sections; however, the theoretical inverse kinematics to successfully navigate the full workspace is outlined in this section. These derivations are assuming that the position of the end-effector is known; resulting in known values for each entry the homogeneous transformation matrix (HTM) found using forward kinematics. With these variables determined, the configuration of each joint preceding the end-effector is known. The HTM can be more easily represented with variables as shown in Figure X where the unknowns are the parameters of the rotational joints θ_2 , θ_4 which are found using the $r_{i,i}$ entries of the HTM. The other unknowns of the prismatic joints are d_1 , and d_3 which can be found using

computed values for θ_2 . Through analyzing the HTM, θ_2 can be found using the d_x and d_y entries of the HTM which are known:

$$\theta_2 = \text{Atan2}(d_x, -d_y)$$

Once θ_2 is computed, θ_4 is found using the $r_{2,1}$ and $r_{1,1}$ entries of the HTM:

$$(\theta_2 - \theta_4) = \text{Atan2}(r_{2,1}, r_{1,1})$$

or

$$\theta_4 = \theta_2 - \text{Atan2}(r_{2,1}, r_{1,1})$$

Also with θ_2 computed, d_3 is found through algebraic manipulation:

$$d_3 = \frac{d_x}{S_2}$$

Likewise, d_1 is simply:

$$d_1 = d_z + 7$$

C. Velocity Analysis

From an implementation perspective, the angular velocity of the end-effector due to each revolute joint can prove useful for determining the pulse rate of the stepper motors and time-to-destination. Because the current Robo-Aide prototype is hard-programmed for solely the prismatic joints, the angular velocity is not a factor. The following derivation is for the theoretical design to be discussed in later sections. The angular velocity can be defined by the equation:

$$S(w_{\theta_2}) = \dot{R}_{z_1} R_{z_1}^T$$

where R_{z_1} is a rotation about the z_1 axis shown in Figure 5.

The matrix R_{z_1} with respect to θ_2 is given as:

$$R_{z_1}(\theta_2) = \begin{bmatrix} \cos(\theta_2) & -\sin(\theta_2) & 0 \\ \sin(\theta_2) & \cos(\theta_2) & 0 \\ 0 & 0 & 1 \end{bmatrix}$$

Therefore, the transpose of $R_{z_1}(\theta_2)$ is:

$$R_{z_1}^T(\theta_2) = \begin{bmatrix} \cos(\theta_2) & \sin(\theta_2) & 0 \\ -\sin(\theta_2) & \cos(\theta_2) & 0 \\ 0 & 0 & 1 \end{bmatrix}$$

and the derivative of $R_{z_1}^T(\theta_2)$ is:

$$\dot{R}_{z_1}(\theta_2) = \begin{bmatrix} -\sin(\theta_2)\dot{\theta}_2 & -\sin(\theta_2)\dot{\theta}_2 & 0 \\ \sin(\theta_2)\dot{\theta}_2 & \cos(\theta_2)\dot{\theta}_2 & 0 \\ 0 & 0 & 1 \end{bmatrix}$$

With these matrices defined, the angular velocity of the end-effector due to the first revolute joint of Frame 1 is given as:

$$\begin{bmatrix} \cos(\theta_2)\dot{\theta}_2 & -\sin(\theta_2)\dot{\theta}_2 & 0 \\ \sin(\theta_2)\dot{\theta}_2 & \cos(\theta_2)\dot{\theta}_2 & 0 \\ 0 & 0 & 1 \end{bmatrix} \begin{bmatrix} \cos(\theta_2) & \sin(\theta_2) & 0 \\ -\sin(\theta_2) & \cos(\theta_2) & 0 \\ 0 & 0 & 1 \end{bmatrix} = \begin{bmatrix} 0 & -\dot{\theta}_2 & 0 \\ \dot{\theta}_2 & 0 & 0 \\ 0 & 0 & 0 \end{bmatrix} \triangleq \begin{bmatrix} 0 \\ 0 \\ \dot{\theta}_2 \end{bmatrix}$$

The angular velocity of the end-effector due to the second revolute joint of frame 3 is found using the same method as frame 1 and results in:

$$\begin{bmatrix} 0 & -\dot{\theta}_4 & 0 \\ \dot{\theta}_4 & 0 & 0 \\ 0 & 0 & 0 \end{bmatrix} \triangleq \begin{bmatrix} 0 \\ 0 \\ \dot{\theta}_4 \end{bmatrix}$$

IV. RESULTS

There were many challenges that our team faced throughout the design and testing process. The initial structure of the design shown in Figure 2 is almost identical to the final design shown in Figure 3. The exceptions include the additional 3-D printed part that was placed at the first revolute joint in an attempt to counter the weight of the horizontal prismatic joint. Another difference between the initial design and final structure is the camera. Although nearly invisible, the pins of the OpenMV Camera M7 are visible at the end of the horizontal prismatic joint in Figure 3 [17]. The camera we received for the project burnt out due to what we believe was a faulty power source. The main challenge we faced involved the design of the first revolute joint. When the horizontal prismatic joint was disconnected, the revolute joint moved the turntable as expected. A video of the working revolute joint is shown in Emb. Video 1. When the horizontal prismatic joint was attached to the revolute joint, at first the gear would slip down the shaft of the motor causing it to spin below the complementary gear attached to the top turntable piece. This was fixed by wrapping tape as a stopper below the gear. However, the stepper motor would then jerk with each pulse. This jerking was caused by the stepper motor attempting to turn, but being unable to as the gear attached to it was unable to turn. After switching all wires, changing code, and switching the revolute stepper motor with the stepper motor for the prismatic arm joint, it was concluded that the cause was that the gear was physically hindered from turning. This jerking only occurred when the horizontal prismatic arm was connected and was lessened so that the joint could turn with assistance when the weight of the arm was manually held up. Therefore, it was concluded that the bend in the metal piece used for the plate holding the arm and the ability of the turntable to become cocked by a few millimeters when

unevenly loaded caused the gears of the revolute joint to become misaligned and thus unable to turn. A solution was designed to add support to keep the plates of the turntable parallel and to stabilize the revolute joint motor as shown in Figure 3. However, this added friction and the gears still behaved as though they were misaligned. The inability to make the revolute joint function caused the theoretical workspace (Figure 2) and the experimental workspace to differ. Since the robotic arm is unable to rotate the entire 360°. The experimental work space was instead a rectangular volume, a slice of the intended revolved rectangle). Therefore, the end-effector can only access a rectangle 12.71 cm tall and 24.13 cm long, matching the maximum ranges of the vertical and horizontal prismatic joints respectively. Only objects in-line with the arm in its home configuration can be accessed. Though the arm cannot rotate, the Robo-Aide is still a free-standing robotic arm that was able to successfully move and retrieve objects and deliver them to a specified location. The two prismatic joints work, and the revolute joint can be manually turned. The end-effector is able to revolve in order to achieve the best angle to grab an object. The current functionality implements a hard-coded movement implementation necessitating that objects be placed consistently. With this constraint, the Robo-Aide is able to autonomously move to, grab, and deliver the placed object. Even with issues in the current design, the Robo-Aide prototype successfully demonstrated the retrieval of a surgical instrument using forward kinematics. A video of our working demonstration is shown in Emb. Video 2.

V. CONCLUSION

The Robo-Aide prototype is able to act as a manipulator that advances the end-effector claw to the position of an object using forward kinematics. For the purposes of this class, Emb. Video 2 of the Robo-Aide only demonstrates a specific and small working motion; however, it can be programmed to reach farther in the vertical and horizontal directions by simply manipulating the parameters of the prismatic joints. In future prototypes, the revolute joint will perform as expected with experimentation in the: weight of the horizontal prismatic joint, meshing of the gears in the revolute joint, and determination of an optimal pulse rate for the stepper motor controlling the revolute joint. Once the revolute joint is operational, an OpenMV Camera M7 will be added in conjunction with a microphone using inter-integrated circuit (I2C) protocol to allow for commands to act as verbal inputs into the system to locate and retrieve objects for the user. This will remove dependency of the user to hard-program the arduino and allow the Robo-Aide to be implemented in non-testing environments, where objects are almost never placed in exactly the same location and orientation. Finally, we plan on implementing a drivetrain for translation around its environment in hopes of the Robo-Aide achieving complete autonomy [18].

REFERENCES

- [1] Author Unknown, "Mobility is Most Common Disability Among Older Americans, Census Bureau Reports," *U.S. Census Bureau*, U.S Department of Commerce.
- [2] M. Mather, "Fact Sheet: Aging in the United States", *Population Reference Bureau*.
- [3] C. Halvorson, "Top 7 Challenges Facing Home Health Agencies in 2013," *Business Growth - For Your Industry*, 13 June, 2013.
- [4] K. Larson, "Top 10 Complaints from Home Care Clients", *Home Care Pulse*,
- [5] M. Geewax, "Discovering the True Cost of At-Home Caregiving," *Morning Edition*, 1 May, 2012.
- [6] B. Romanik, "Coming Soon: Personal In-Home Robots ,," *Techwell Insights*, 30 June, 2017.
- [7] M. Santora, "For Surgery, an Automated Helping Hand," *The New York Times*, 18 January, 2005.
- [8] Author Unknown, "The robot should be able to do everything a nurse can...," *The Truth About Nursing*, 18 January, 2005.
- [9] M. Dougherty, "Intelligent Robot Scrubs In," *Invivo*, Columbia University Medical Center, Columbia University, 26 January, 2004.
- [10] Mithun George Jacob, Yu-Ting Li, Juan P. Wachs, "Gestonurse: A Multimodal Robotic Scrub Nurse", 7th ACM/IEEE International Conference on Human-Robot Interaction (HRI), March 5-8, 2012
- [11] Author Unknown, "LRS-350 Series", *Sager Power Systems*, Mean Well, Accessed 21 April, 2018.
- [12] Arduino, "Arduino Mega 2560 Rev 3", *arduino.cc*, Accessed 14 March, 2018.
- [13] Adafruit, "Adafruit Motorshield v2.3", *adafruit.com*, Accessed 14 March, 2018.
- [14] Arduino IDE, "Arduino Software", *arduino.cc*, Accessed 14 March, 2018.
- [15] Nema 23 Stepper Motors, "Nema 23 Bipolar", *omc-stepperonline.com*, Accessed 14 March, 2018.
- [16] TB6600 Stepper Motor Drivers, "TB6600 Stepper Motor Driver SKU: DRI0043", *dfrobot.com*, Accessed 21 April, 2018.
- [17] Author Unknown, "OpenMV Camera M7", *https://openmv.io*, Accessed 14 March, 2018.
- [18] B. Bennet, "Drivetrain Design - Featuring the Kitbot on Steroids", *www.simbotics.org*, Accessed 21 April, 2018.



